Laser disintegration of Van der Waals clusters of carbon-containing molecules

E. S. Toma and H. G. Muller
FOM-Institute for Atomic and Molecular Physics, Kruislaan 407, 1098 SJ Amsterdam, The Netherlands
(Received 13 December 2001; published 18 July 2002)

We report the production of highly charged ions, C^{5+} and O^{6+}, obtained by Coulomb explosion of propane and, respectively, carbon dioxide clusters, exposed to laser pulses of $(1-6)\times10^{14}$ W/cm^2 intensity. At such intensities, only triply charged ions were created via tunneling ionization of isolated molecules. Carbon ions with energies of 1.2 keV and oxygen ions with energies of 2 keV have been detected. Some information about the explosion dynamics could be extracted from numerical simulations.

DOI: 10.1103/PhysRevA.66.013204 PACS number(s): 36.40.−c, 52.50.Jm, 52.65.Cc

I. INTRODUCTION

Interaction of strong laser fields with atoms or molecules has been a major area of interest in atomic physics for the past decades. For long-wavelength radiation, in the near-infrared domain, the main ionization mechanism for intensities lower than 10^{14} W/cm^2 is multiphoton ionization via intermediate states. At higher intensities, the strong electric field can distort the atomic potential, lowering the barrier enough to make the electron able to tunnel through it [1]. Tunneling becomes dominant as soon as the Keldysh parameter $\gamma=\sqrt{I_p/(2U_p)}$ is smaller than 1 [2]. In this expression I_p is the ionization potential of the atom (or ion) and U_p is the ponderomotive energy given in eV by $9.33\times10^{-14}I$ (W/cm^2)$\lambda^2(\mu$m$^2)$. The electron is even able to escape over the barrier for intensities larger than I_{OTBI} (W/cm^2)$=4\times10^9[I_p(\mathrm{eV})]^4/Z^2$, where Z is the charge state of the relevant ion [3]. For single charged ions I_{OTBI} is of the order 10^{14}–10^{15} W/cm^2, but it becomes very high ($>10^{18}$ W/cm^2) for the production of highly charged ions, when removal of an inner-shell electron is required.

Because of their high local density and their efficient absorption of laser energy, clusters offer an attractive alternative to atoms or molecules as a target substance for the creation of high-charge ionic states at much lower intensities than required by optical-field-induced (OFI) ionization of atomic gases. Many studies have been performed on noble-gas clusters, using short and intense laser pulses, concerning both ion and electron production, as well as radiation emission [4–6] and even production of fusion neutrons [7]. Ions with maximum energies of 1 MeV have been reported at laser intensities of $\simeq10^{16}$ W/cm^2, charged as high as 40+ for Xe, or 25+ for Kr [8–10]. Such ions were obtained from the explosion of clusters of less than 2500 atoms. Only Xe^{8+} and Kr^{8+} can be produced at 10^{16} W/cm^2 via over-the-barrier ionization of atoms. At the same intensities, electron spectra revealed the production of hot electrons, whose energies peak at 2.5 keV, besides slower ones, with energies less than 1 keV [10,11].

The dynamics of cluster explosions has received considerable attention up to date. Various models were proposed to explain the high-charge states obtained in different experimental conditions and the nonthermal x-ray emission. Thompson *et al.* advanced the idea of coherent electronic motions in the strong laser field as being responsible for an enhanced probability of multiple ionization from an inner shell [12]. Such motions then caused production of highly charged ions (Xe^{48+} and Kr^{27+}), which decay emitting x-ray radiation of 4–5 keV, in experiments performed with ultraviolet radiation at high intensities (10^{19} W/cm^2) [4,13]. In the ionization-ignition model the field of the neighboring ions, created in the initial ionization events, assists the laser in lowering the ionization barrier, thus igniting the cluster to undergo further ionization [14,15]. This model predicts very little dependence of the charge distribution on the cluster size, and it is only applicable to small clusters.

Classical simulations including both electron and ion dynamics proved that the space charge of the ions retains a significant fraction of ionized electrons in the core of a 55-atom cluster, diminishing the importance of ion-ion interactions and supporting the idea of treating the cluster as a nanoplasma [16]. According to the hydrodynamic model developed by Ditmire *et al.* [10,17] collisions between ions (created initially by OFI ionization in low-charge states) and laser-driven electrons form the main mechanism for the further ionization of ions and heating of the electrons. The cluster will expand because of the pressure the free electrons exert on the ions. The fastest electrons will evaporate from the cluster [11], leaving the core positively charged. The heating is enhanced as soon as the electron density reaches three times n_{crit} (the density at which the laser frequency equals the plasma frequency). Experimental results showing that at a given cluster size (10^5–10^6 atoms for that experiment) there is an optimum pulse width for maximum absorption of laser energy, provide strong evidence for such resonant heating [18]. The ions will rapidly be ionized to high-charge states by the hot electrons. The combined action of the repulsive Coulomb forces between ions and the hydrodynamic pressure associated with the hot electrons will make the cluster explode. The electrons cool as they give some of their energy to the ions. The Coulomb pressure is more important for clusters of 2000 atoms or smaller, which do not retain much of the electrons [10]. For larger clusters, the hydrodynamic expansion dominates, except for a short time after resonance, when the high electrostatic field (built up in the cluster because of the fast escape of the heated electrons) pulls the cluster apart, creating very energetic ions [19]. The big clusters expand more slowly, absorb more energy from the laser, and produce ionic states of higher charge in the expansion process.

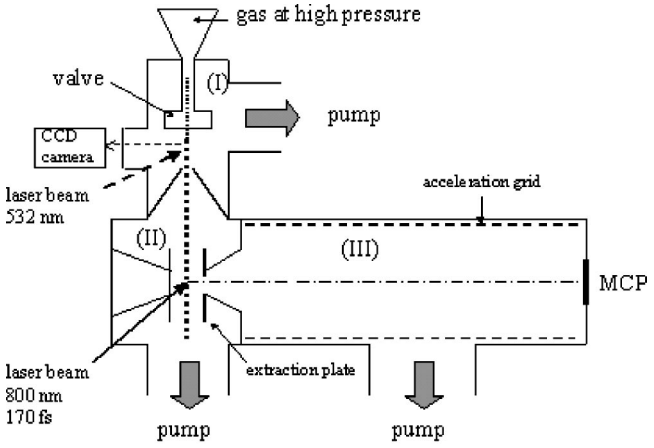

FIG. 1. Schematic of the experimental setup. (I) is the expansion chamber, where the clusters are formed. For the Rayleigh-scattering measurement the beam of a Nd:YAG laser was sent on the cluster jet, 5 mm below the valve, and the scattered light was detected on a CCD camera. The spectrometer consists of the interaction chamber (II), where the infrared laser irradiates the clusters, and the time-of-flight tube (III), where the ions are detected.

Molecular clusters have received little attention up to now, in spite of the advantage they offer of studying elements that are hard to cluster in pure form [14,20,21]. We focused our attention on clusters of carbon-containing molecules: carbon dioxide (CO_2) and propane (C_3H_8). K-shell ionization of carbon ions via barrier suppression requires laser intensities higher than 2.6×10^{18} W/cm^2 because of the deep ionization potentials of C^{4+}(392 eV) and C^{5+} (490 eV). As shown for noble gases, a gas of clusters can very much lower the intensity needed for production of high-charge ions. Previous experiments produced fair amounts of C^{4+} at intensities around 10^{15} W/cm^2, from small acetone clusters [14] and C_{60} [22]. Using big clusters as target, we exposed carbon atoms to low laser intensities (of the order 10^{14} W/cm^2), which, according to the equation for I_{OTBI}, can create at most doubly charged ions by tunneling ionization of carbon atoms. From the ion spectra, we also extracted information about the dynamics of the explosion.

II. CLUSTER-SIZE DETERMINATION

Figure 1 presents a schematic of our experimental setup. A titanium:sapphire laser was used for the experiment, working at a repetition rate of 10 Hz. The characteristics of the pulse were 800 nm central wavelength and 170 fs duration, with pulse energies up to 6 mJ. The clusters were created in an adiabatic expansion that took place in a chamber installed on the top of an electron spectrometer, which could also be used for time-of-flight measurements on ions. A mixture of helium and a carbon-containing gas at high backing pressure (up to 30 bars) was made to flow into the low-pressure expansion chamber (10^{-7} mbars background pressure) by a pulsed, solenoid-controlled valve synchronized with the laser. Only the central part of the jet could pass into the spectrometer through a skimmer that was placed between the chambers, 2 cm below the nozzle.

The interaction of the laser beam with the clusters took place between the two extraction plates depicted in the figure by thick lines, in the interaction chamber of the spectrometer. The ions were detected in the time-of-flight chamber (1 m long) by a multichannel plate (MCP) connected to a computer through an oscilloscope, after being extracted from the interaction region and accelerated towards the MCP by negative voltages of 80 V on the plates and 2500 V on the flight tube. The solid angle that the spectrometer accepts is quite small, and is inversely proportional to the initial kinetic energy of the ions. Only particles with a velocity component in the direction of the detector can enter the flight tube, because the extraction voltage is not large enough to turn around ions that go in the opposite direction. In addition, the perpendicular velocity of the ions should not be larger than 1% of the total velocity they acquire in the flight tube, otherwise they will miss the 2-cm MCP.

Condensation in the free jet expansion produces Van der Waals clusters of sizes that depend on the gas source parameters: pressure, temperature, and nozzle size. In the absence of a general condensation theory that would exactly predict the average cluster size for a given set of initial expansion conditions (p_0, T_0, d), empirical scaling laws were developed in order to correlate flow fields that are similar with respect to cluster formation or other expansion characteristics such as terminal temperature. Through the concept of corresponding jets [23,24] the scaling parameters have been extended for expansions of different gases [25,26].

The scaling of the cluster size with the conditions of expansion is given by the Hagena parameter:

$$\Gamma^* = k(C_\gamma d/\tan\alpha)^q p_0 T_0^{-r},$$

where d is the diameter of the nozzle, α is the expansion half-angle (45° for sonic nozzles), C_γ is a γ-dependent factor [24] (1 for sonic nozzles), p_0 is the source pressure, T_0 is the initial gas temperature, and $k = r_{ch}^{3-q} T_{ch}^{r-1}/k_B$.

In order to correlate rare gases with metals, the characteristics were defined as

$$r_{ch} = (m/\rho)^{1/3} \quad \text{and} \quad T_{ch} = \Delta h_0^0/k_B,$$

where m is the atomic mass, ρ is the density of the solid state, and Δh_0^0 is the sublimation enthalpy per atom at 0 K [25,26].

The parameter r gives the scaling power of T_0 with p_0 for the same cluster size, when the nozzle diameter is not changed, and is related to the q parameter, which represents the scaling power of d with p_0 for the same output at constant source temperature, by the expression $r = \gamma/(\gamma-1) - [(2-\gamma)/2(\gamma-1)]q$ (where γ is the adiabatic constant of the gas) [27]. The value of the q parameter is within 0.5 and 1, and can be determined precisely only from cluster-size measurements. Experimental results give $q = 0.85$ for rare gases and metal vapors, and $q = 0.6$ for CO_2 [23,27].

Based on experimental data, it is possible to affirm that the formation of clusters occurs if Γ^* exceeds 200, and that

the clusters contain 100 atoms for $\Gamma \sim 1000$. The average cluster size is proportional to $(\Gamma^*)^f$, with $2 \leqslant f \leqslant 2.5$ [17,26,28]. Very big clusters of 10 000 atoms (100 Å) were observed for $\Gamma^* > 50\,000$ [29].

It is difficult to experimentally determine the size of the clusters. We have applied the Rayleigh-scattering technique, which gives, in principle, information about the average size of the clusters. The Rayleigh-scattering partial cross section is $\sigma(\lambda, \theta) \sim R_c^6(1+\cos^2\theta)/\lambda^4$, where R_c is the cluster radius, λ is the scattered-light wavelength, and θ is the scattering angle. If n_c is the cluster density, the scattered signal S is proportional to $n_c\sigma$. Considering the expression for σ and the fact that R_c is proportional to $N_c^{1/3}$, N_c being the average number of atoms per cluster, we have $S \sim n_c N_c^2$. If all atoms condense into clusters, $n_c \simeq n_0/N_c$ and we can write $S \sim N_c p_0$, where n_0 and p_0 are the density and the pressure in the gas reservoir. If S scales as p_0^{f+1}, the average cluster size increases as p_0^f, with $2 \leqslant f \leqslant 2.5$, as measured in many experiments that have applied this technique [6,10], confirming the result mentioned in the discussion about the Hagena parameter. (If no clustering occurs, S is simply proportional to p_0.)

We performed the measurements at room temperature ($T_0 = 300$ K) using a nozzle of $d = 500$ μm and $\alpha = 45°$, and the only expansion parameter we could manipulate was the backing pressure p_0. The beam of a Nd:YAG (yttrium aluminum garnet) laser at the second-harmonic wavelength (532 nm, 6 ns, 20 mJ) was focused on the gas jet in the expansion chamber, 5 mm under the nozzle, by a lens of 250 mm focal distance. At this distance the collision frequency has dropped 10 000 times compared to immediately after the nozzle, the condensation process stopped, and the clusters flow free at terminal velocity [30]. Light scattered on the jet was detected at 90° by a calibrated charge-coupled device (CCD) camera. Reflections of the laser beam on the windows were blocked by pinholes and the chamber walls were painted black in order to minimize the background signal.

The measurements were done initially on pure CO_2 and pure propane. In the case of propane, there was no scattered light detected for p_0 varied from 1 to 7 atm, so it can be concluded that no clustering occurred for this gas at these pressures. (For propane at room temperature, the phase transition to liquid takes place at $\simeq 8$ atm.) In the same range of pressures, the CO_2 forms small clusters, with a size of 120 molecules at 10 atm. N_c was found to be proportional to p_0^3, a somehow large value for the power factor.

The difficult part in this measurement was the estimation of the proportionality constant between the scattered signal and the cluster size, because the signal given by individual atoms was below the detection limit. In $S = CN_c p_0$ the constant C is dependent on the detector sensitivity, on the light intensity, and on the polarizability of the molecules. We estimated C from theoretical considerations for the pure gas from the expression $Cp_0 = N_{\text{tot}} n \sigma_m las$, where N_{tot} is the total number of photons in the laser pulse at the energy of reference, n the gas density in the focus, σ_m the molecular scattering cross section at 90°, l the length of the focus, a the steric angle that hits the camera objective, and s the camera sensitivity in millivolts per photon. The camera sensitivity was determined by exposing the CCD chip to an isotropically scattered laser pulse of known energy. Then we could calculate it at different concentrations and beam energies according to $C_{x\%} = x\% \times C_{\text{pure}} E_{\text{reference}}/E_{\text{beam}}$. The main error comes from the estimation of the gas density in the jet and translates into a relative error of $\approx 50\%$ in the average cluster size.

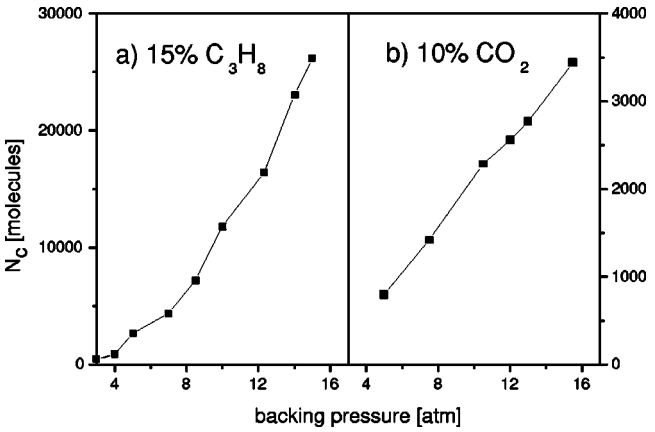

FIG. 2. Average cluster size at different p_0, derived from the Rayleigh-scattered signal, for propane (a) and carbon dioxide (b). Both gases have been mixed with He in the gas reservoir, in concentrations indicated in the figure. $N_c \sim p_0^{2.5}$ for propane, and $N_c \sim p_0^{2.3}$ for CO_2.

For rare gases, it was observed that the less ''ideal'' the gas (the higher the critical-point temperature, for example), the higher the nucleation rate is [29]. Xe clusters better than Ar, and He forms clusters only at very low source temperatures. Pure propane is a very poor gas from the condensation point of view, although it has a higher critical temperature than CO_2 or Xe. But it should not be forgotten that it has a smaller adiabatic constant ($\gamma_{CO_2} = 1.3$, $\gamma_{C_3H_8} = 1.14$, also at 1 atm). For the same initial conditions, a gas of higher γ will cool faster than a gas of lower γ.

The formation of clusters can be enhanced by the addition of a carrier gas, usually a light, monatomic gas. The mixture is meant to increase the adiabatic constant and to reduce faster the temperature, thus increasing the collision frequency of the expansion. It also makes possible the use of higher backing pressures than allowed by the thermodynamic properties of the seed gas. The γ constant of a mixture of He and propane, containing propane in a proportion of 15%, is 1.4, and at 2 nozzle diameters distance from the nozzle the density is twice higher than in the case of pure-propane expansion. Mixed with He, propane does form clusters starting from very low backing pressures, and reaching a value of 25 000 molecules per cluster at 15 atm [Fig. 2(a)]. N_c scales proportional to $p_0^{2.5}$. As the clusters grew larger with p_0, the scattered signal increased above the saturation limit of the detector sensors, and the energy in the incident beam had to be reduced. The attenuation was taken into account in the calculation of N_c.

Mixing with He also improves the results for CO_2: the onset of clustering falls to around 3 atm, and the power law

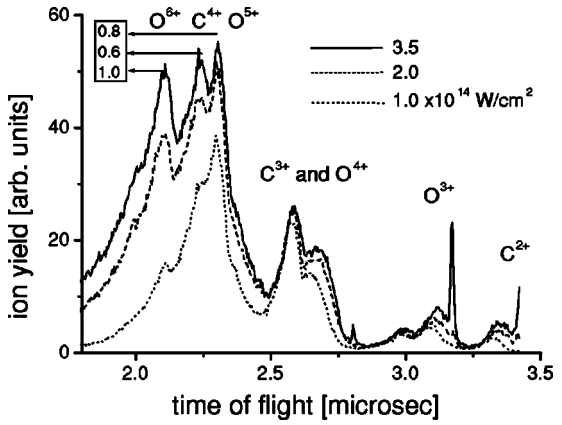

FIG. 3. Ion spectra from Coulomb explosions of CO_2 clusters of $\simeq$4500 molecules, at different laser intensities: 10^{14} W/cm^2 (dotted line), 2×10^{14} W/cm^2 (dashed line), and 3.5×10^{14} W/cm^2 (solid line). The inset in the upper left corner shows, in keV, the kinetic energies of the most important ions at the peak position.

changes to $N_c \sim p_0^{2.3}$. Clusters containing more than 3000 molecules are obtained beyond 14 atm [Fig. 2(b)]. The cluster size is much lower as compared to a mixture of propane and He in spite of the higher γ. The reason might be the higher number of atoms contained in the molecule of propane, which increases the number of degrees of freedom per molecule, thus allowing a more rapid dissipation of the heat of cluster formation.

Unfortunately, apart from the average size, nothing can be learned about the cluster size distribution from the Rayleigh-scattered light measurements. If there is a significant fraction of the molecules that do not form clusters, the clusters that are present might have typical sizes much different from the average.

III. CLUSTER EXPLOSION

The central part of the jet passes through a skimmer with a diameter of 2 mm into the chamber where the interaction with the laser takes place. The skimmer cuts the wings of the jet, preventing the occurrence of frontal shock waves, and transmits further only a small amount of gas, thus maintaining a low pressure in the interaction chamber, 10^{-5} mbars on average. We shall discuss the results obtained for CO_2 and propane in two separate sections.

A. CO_2

We took ion spectra from disintegration of CO_2 clusters, changing either the conditions of expansion or the characteristics of the laser pulse. The clusters were formed in an expansion of CO_2 mixed with He in the proportion of one part in ten. At 20 atm backing pressure the average cluster size is 4500 molecules, as given by the Rayleigh-scattering measurement. The spectrum depends critically on the intensity (Fig. 3). At 10^{14} W/cm^2 only two peaks are visible, each formed by the contribution of two ions, C^{3+} and O^{4+} (that have the same mass/charge ratio and are indistinguishable in a time-of-flight measurement), and, respectively C^{4+} and O^{5+} (which could not be separated at our resolution). The O^{6+} peak clearly emerges from the wing of its neighbor peak at 1.5×10^{14} W/cm^2.

The calibration of the spectra with time was done on the H_2O^+ peak, produced by ionization of the water molecules present in the background gas, and still visible when the valve is closed. The water molecules have very small initial velocities, and this calibration gives us information on the arrival time of ion species with zero initial kinetic energy. The detection method is such that we cannot distinguish between ions of the same m/q ratio. The time scale also contains information about the kinetic-energy distribution of the ions, in their displacement from the zero-velocity position. It is essential that the peaks do not overlap each other too much, in order for this information to be extracted unambiguously. The spectra were accumulated for 200 shots and the average peak intensity was measured with a calibrated photodiode. The calibration was done in a separate measurement on the ionization threshold of He^+. As the intensity increases, the signal gets stronger, but does not change in structure. Saturation is reached at 5×10^{14} W/cm^2.

The very narrow peaks at 3.2 and 2.8 μs are due to ions of O^{3+} and, respectively, C^{3+} produced with almost zero initial velocity by direct OFI ionization of isolated molecules. These peaks appear at lower intensities than I_{OTBI} expected for atoms: O^{3+} at 2×10^{14} W/cm^2, C^{3+} at 3.5×10^{14} W/cm^2. The ions produced by Coulomb explosion appear at shorter times of flight and form broader peaks. By explosion, they are expelled with high initial velocities from the potential well caused by the evaporation of hot electrons. The excess kinetic energies at the peak indicate an average potential drop of 170 eV as ions depart to infinity. It acts differently on ions of different charge and this might explain why the C^{3+}-and-O^{4+} peak has a shoulder. The fastest ions are expected to come from the surface of the cluster, where electric fields are the strongest. The spectrum measured at 3.5×10^{14} W/cm^2 shows O^{6+} ions of more than 2 keV, suggesting a maximum potential of around 300 eV at the surface of the expanding cluster. Because the peaks overlap, it is not possible to analyze each charge state individually.

A measurement of the ion spectrum at different backing pressures, 10 and 20 atm, reveals no change in the structure of the spectrum when increasing the average cluster size from 2000 to 4500 atoms.

B. C_3H_8

For the results presented in Fig. 4, the measurement was done on clusters of 50 000 molecules on average, obtained from a mixture of 15% propane at $p_0=20$ atm. The ion spectrum from ionization of propane clusters shows carbon ions up to a charge state of 5+ and a peak corresponding to H_2^+. The very narrow peaks correspond to ions created by direct OFI ionization. The ions from the much broader peaks are produced by the Coulomb explosion of the laser-heated clusters. For the intensity measurement we did binning on a calibrated photodiode signal.

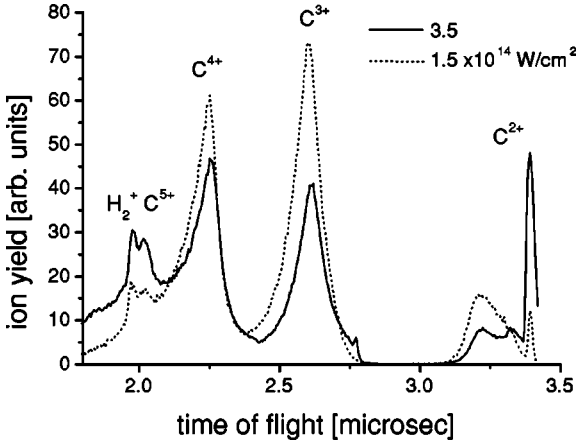

FIG. 4. Ion spectra from Coulomb explosions of propane clusters of $\simeq 50\,000$ molecules at two laser intensities: 1.5×10^{14} W/cm^2 (dotted line) and 3.5×10^{14} W/cm^2 (solid line).

With only one mass present in the spectrum the peaks are fairly well separated, and it is relatively easy to plot the number of ions per charge state as a function of intensity (see Fig. 5). C^{5+} appears as a distinct peak at $\simeq 10^{14}$ W/cm^2. As the intensity increases, the amount of C^{4+} and C^{5+} is also increasing up to a saturation point after which it is slowly decreasing as the clusters are destroyed faster by the more intense laser. At 6×10^{14} W/cm^2 the amount of C^{5+} is $\simeq 50\%$ that of C^{4+}. What happens after saturation is expected to be very dependent on the exact temporal pulse shape and focus geometry. Both of these are poorly known in our experiment, so we cannot draw any conclusion from the slight decrease of the ion signal in Fig. 5, at higher intensities.

The peaks of Fig. 4 could be also analyzed individually with respect to the energy of the ions. In Fig. 6 the peaks corresponding to three charge states 2+, 3+, and 4+, were plotted as a function of energy at the same intensities as in Fig. 4. A small correction was done in these graphs, for the fact that the acceptance angle of the spectrometer is smaller for ions of higher velocities. The C^{4+} ions acquire in the explosion, energies of more than 1.2 keV, indicating a potential of 300 V at the surface of the cluster. The average charge

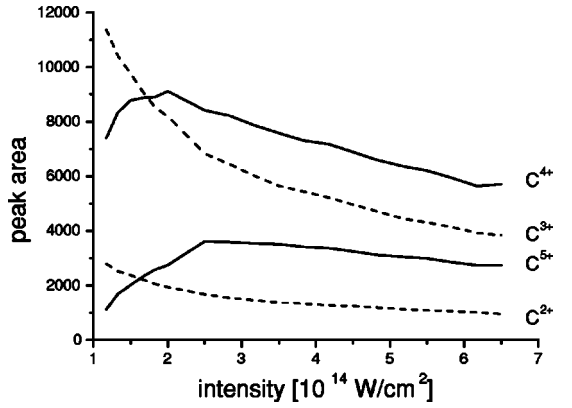

FIG. 5. C^{n+} amount at different intensities, obtained from the ion spectra by integration of the corresponding peaks.

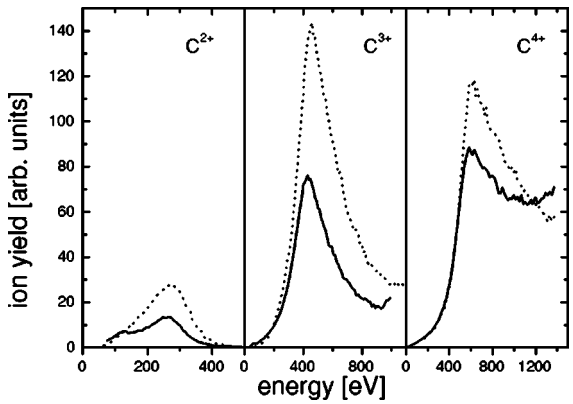

FIG. 6. The peaks of C^{2+}, C^{3+}, and C^{4+} (from left to right) as a function of energy, at 1.5×10^{14} W/cm^2 (dotted line) and 3.5×10^{14} W/cm^2 (solid line).

per ion is $\simeq 3.5$. If all electrons were to leave the cluster, the radius of the sphere creating this potential would be 2.5 μm, 125 times bigger than the initial cluster size. The cluster would reach this dimension only a few pulse durations after the pulse, which means that most of the free electrons were actually trapped in the cluster during the expansion, otherwise we would have seen higher ion energies in the spectrum. This implies the dominance of the hydrodynamic pressure in the process.

Electrons with kinetic energies lower than 300 eV cannot leave the potential well. They are left in the cluster volume, oscillating in the laser field. An electron of T_0 initial kinetic energy (gained by backscattering on ions) can get from the laser field an extra energy of maximum $\sqrt{8U_pT_0}$, which for $T_0=300$ eV, makes a total of 500 eV at 3.5×10^{14} W/cm^2. This can create even C^{6+} by collisional ionization.

IV. THEORETICAL MODEL OF THE EXPLOSION

To help interpreting the experimental results, we ran some numerical simulations of the propane-cluster explosion, using the simple classical model introduced by Ditmire [16]. We assumed that the exact initial location of the carbon atoms would not affect the later stages of the explosion very much. The carbon atoms were therefore arranged in a spherical subset of an fcc lattice, with lattice constant 4.7 Å. The proper volume of each atom is then 40 Å^3, which gives them the same density as in liquid propane. We considered only the carbon and neglected the protons. Initially only neutral atoms were filling the particle array, and free electrons added to the array later, as they were created by ionization. For each created electron, the charge state of the parent atom (or ion) was changed accordingly. The program calculates the total electric field at the position of each particle, and uses these values in the check for ionization events, and in determining the motion of the particles.

The instantaneous value of the laser electric field and the Coulomb-field value at the atom (ion) determine the conditions for ionization. The ionization can take place by tunnel-

ing or by inelastic collisions with (sufficiently fast) electrons. This last case was allowed to occur only if the impacting electron passes closer than 2.12 Å from the ion (distance representing the radius of the proper volume), with a probability that reflects the corresponding cross section. To this end we assumed that the target atom (or ion) was ionizing at a constant rate as long as a fast electron was within its proper volume. This collisional-ionization rate is given by the product of the Lotz cross section [31] with the relative velocity (extrapolated to its asymptotic value), divided by the proper volume. The expression of the Lotz cross section is, with a small approximation,

$$\sigma_L = a_L N_e \frac{\ln(K/I_p)}{K I_p},$$

where $a_L = 450$ (eV)^2 Å^2, N_e is the number of electrons in the outer shell of the ion, K is the center-of-mass energy, and I_p is the ionization potential of the ion [32].

The rate for tunnel ionization by the laser field is given by a more complex expression [17,33]:

$$W_t = \mathcal{F}\frac{(2l+1)(l+|m|)!}{2^{|m|}|m|!(l-|m|)!}\left(\frac{2e}{n^*}\right)^{2n^*}\frac{I_p}{2\pi n^*} \times\left(\frac{2(2I_p)^{3/2}}{E}\right)^{2n*-|m|-1}\exp\left(-\frac{2(2I_p)^{3/2}}{3E}\right)$$

in atomic units, and where $\mathcal{F}$ denotes a constant factor, E is the total field (laser+interaction) at the ion position, $e = 2.7183$, n^* is the effective principal quantum number ($n^* = Z/\sqrt{2I_p\ (\mathrm{eV})}$), Z being the core charge), l and m are the orbital and the magnetic quantum numbers. For $l = 0$, $\mathcal{F} = 1$, and for $l = 1$, $\mathcal{F} = (n^* - 1)/(n^* + 1)$. The rate is averaged over m for the $2p$ shell. At an intensity of 3.5×10^{14} W/cm^2 the tunneling rate for neutral carbon is 0.83 fs^{-1}, 0.11 fs^{-1} for C^+ and zero for all the other ionic states.

The electric field used in the expression for the tunneling rate was the combined field of the laser and the ions and electrons in the cluster. It was assumed that the distance to these other charges was for the largest part of the explosion large enough that over the distances relevant for tunneling such fields are sufficiently homogeneous to allow the use of the tunneling formula: due to their mutual repulsion ions never approach each other very closely. Electrons entering the proper volume of an atom could potentially create very high and inhomogeneous fields for which application of the tunneling formula would certainly not be justified; for this reason, tunneling was completely suppressed if there was an electron within this proper volume, the rate at those times being purely derived from the Lotz formula. The ionization probability during a time step of the numerical simulation is given by the product of the ionization rate and the time-step duration, $\delta t = 0.0024$ fs in our calculations. Whether ionization takes place or not is decided by comparison with a random number between 0 and 1. (Atomic units were used in the program.)

We did calculations for a cluster of 1500 carbon atoms (to which free electrons added to more than 9000 particles in total) irradiated by a sine-squared laser pulse of 160 cycles total duration. The algorithm used to calculate the motion of the particles is of the ''leap-frog'' type: the positions at time t were used to calculate the forces involved in the updating of velocities from $t - \delta t/2$ to $t + \delta t/2$, and the updated velocity was then used to calculate the new positions at time $t + \delta t$.

The most expensive part of the simulation, in terms of computational time, was the calculation of the Coulomb-force field. Because of the long-range nature of the Coulomb forces every pair of particles had to be taken into account. The duration of the force calculation thus scales proportionally to the square of the number of particles N. The interaction between particles i and j was modeled by a soft-core potential of the form $1/\sqrt{r_{ij}^2 + a_i + a_j}$, where a_i is a constant depending on the identity of particle i. An a constant was attached to each electron (the same for all of them) and ion (depending on the charge state), such that the value of the interaction term between an ion and an electron at $r_{ij} = 0$ equals the ionization potential of the respective ion. The square root and the division required to calculate the forces make this step, which already has the most unfavorable N scaling, also computationally demanding. Using vector instructions available on the newer generations of CPUs made it possible to do the calculations for a 1500-particle cluster in a few days, which was considered the practical limit.

We used in the calculations a sinusoidal laser field (linearly polarized) with a sine-squared envelope, of 2.66 fs optical period, and 150 fs full width at half maximum (FWHM). We ran the calculations for a peak intensity of 3.5×10^{14} W/cm^2. The cluster contains 1500 carbon atoms (500 propane molecules), and the initial radius is 26.5 Å. The laser pulse starts at 0 fs and lasts for 426 fs, with the maximum intensity of 3.5×10^{14} W/cm^2 at 213 fs. Describing the process chronologically, we notice from Fig. 7 that the ionization starts after 100 fs from the beginning of the pulse, and for almost 50 fs most of the electrons are trapped inside the cluster. At this time, the resonant heating of the electrons begins, after the density dropped from a maximum of 3.8×10^{22} cm^{-3} to the critical value of 1.6×10^{22} cm^{-3}, because of the expansion. The large number of electrons present inside the cluster points to an expansion triggered by the hydrodynamic pressure. The average charge state stays constant for a short while (4+), till the electrons get enough energy to further impact ionize the ions. (In fact, only 5% of the total number of free electrons is a result of tunneling ionization.) Slowly, the hot electrons are leaving the cluster volume, but 40% of the total number does not have enough energy to overcome the potential barrier. The average kinetic energy of the trapped electrons reaches a maximum of 300 eV, including the ponderomotive energy, at $t = 200$ fs, when the pulse intensity is close to maximum. By this time the final average charge state is reached (5.12+). (The electrons have a Boltzmann distribution of their energies.) From now

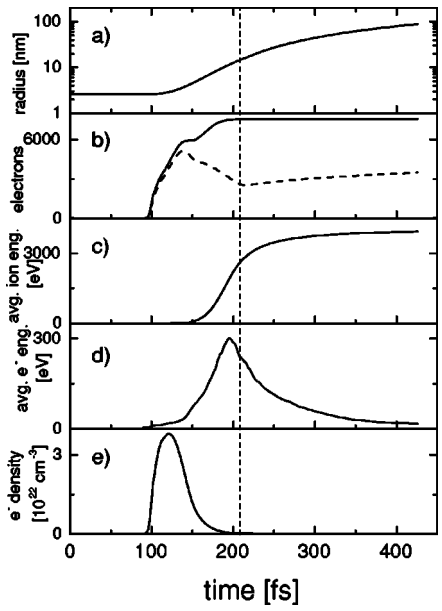

FIG. 7. Results of numerical simulations for a 1500-atom cluster and a pulse of 3.5×10^{14} W/cm^2 peak intensity and 150 fs FWHM. The graph represents as a function of time: the radius of the cluster (a), the total number of free electrons (solid line) and the number of free electrons trapped inside the cluster (dashed line) (b), the average kinetic energy of the ions (c), and of the trapped electrons (d), and the electron density inside the cluster (e). The vertical dashed line marks the peak of the laser pulse.

on the electrons get colder, most of them are outside the cluster, and the expansion is mainly due to the Coulomb repulsion between ions. It can be deduced that the pulse duration is close to optimum for this cluster size. Calculations done using a pulse of 56 fs FWHM showed a 1.5 times smaller maximum of the average electron energy, reached after the peak-intensity moment. Calculations done for a cluster of 620 atoms, using our pulse of 150 fs FWHM, gave a maximum average energy of only 220 eV for the trapped electrons, and a final average ionic state of only 4.4+.

Some electrons that have left the cluster still feel the attraction of the cluster's positive charge and do not depart far from it. They are reincorporated in the cluster by expansion, but their number is quite small, around 500. The cluster radius at $t=426$ fs is 890 Å, and the cluster charge is 4072+. After a maximum of 950 V at $t=180$ fs, the potential at the surface of the cluster decreases rapidly to only 70 V at the end of the pulse. The final average energy of the ions is 3.9 keV. The saturation has been reached soon after the peak of the laser pulse, which indicates that mainly the hydrodynamic expansion is responsible for the high ion velocities. At the end, 33% of the ions are C^{6+} (in contrast to the experimental data, where no distinct peak corresponding to C^{6+} was measured), 46% C^{5+}, and the rest C^{4+}. It shall be stressed that we used a spatially homogeneous pulse in the calculations, which was not the case in the experiment.

The results from the calculation look quite different from those of the experiment. The main difference, however, is caused by the fact that the experiment integrates over a large range of intensities present in the laser focus, the lower intensities being much more abundant than the higher ones. The focal volume as a function of intensity is described by

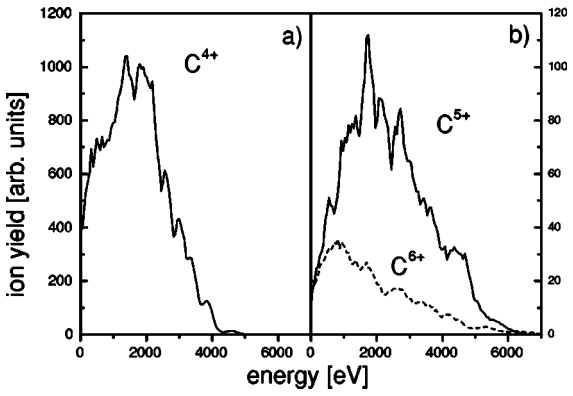

FIG. 8. Peak profiles resulting from averaging numerical calculations run at different intensities, for charge states: 4+ (a), 5+ and 6+ (b).

$$dV(I)\sim\frac{1}{I}\sqrt{\frac{I_0}{I}-1}\left(\frac{I_0}{I}+2\right)dI,$$

where I_0 is the maximum intensity. To simulate such focal volume, we also ran calculations at six smaller intensities: 0.29, 0.35, 0.44, 0.66, 0.88, and 1.75×10^{14} W/cm^2. Nothing happens in the numerical simulations if the intensity is lower than 0.25×10^{14} W/cm^2. The integrated results can be seen in Fig. 8. The energy distributions of the main charge states (4+ and 5+) peak between 1.5 and 1.8 keV, indicating an average potential of 350 V at the surface of the cluster. (The experimental peaks depicted in Fig. 5 suggest a slightly lower potential of 300 V.) The profiles are much more similar to those measured in the experiment. The tails of the some peaks stretch beyond 3 keV. In the experimental spectrum these tails could not be distinguished from the peaks corresponding to higher-charge ions. All these numbers are closer to the experimental results than the values obtained from the peak-intensity calculation. With the volume integration, the number of C^{4+} ions produced is ten times larger than the number of C^{5+} and thirty times larger than C^{6+}. In the experiment, we measured a C^{5+}:C^{4+} ratio of 40% at 3.5×10^{14} W/cm^2. The amount of C^{3+} given by the calculations is far less than that measured, and the maximum energy of these ions is only 200 eV.

It is interesting that the C^{6+} yield peaks at 1 keV, which might suggest that the highest-charge ions are not created at the surface of the cluster, but somewhere inside the cluster volume, in a region where less fields are present. From Fig. 9(b) we can see that by the end of the pulse (when no ionization takes place anymore), the C^{4+} ions are only present at the surface of the cluster, while C^{6+} ions are distributed over the entire volume. These results are obtained at 3.5×10^{14} W/cm^2. At the surface of the cluster the electron energy is lower, because the hottest electrons have either escaped the cluster or have been attracted towards the center of the potential well, and the C^{4+} ions can survive ionization.

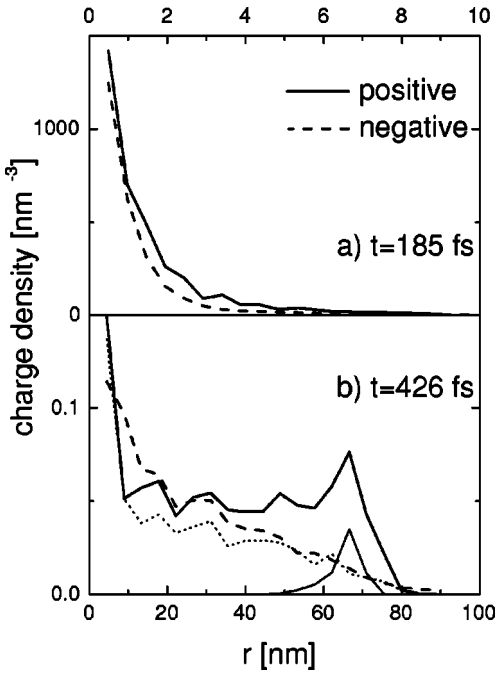

FIG. 9. Positive- and negative-charge densities at two different moments of time: 185 fs from the beginning of the laser pulse (a), and at the end of the pulse (b). The pulse intensity is considered spatially homogeneous with a peak value of 3.5×10^{14} W/cm^2. r is the distance from the cluster's center. In the lower graph (b), in thin lines, the contributions of only 4+ ions (solid) and 6+ ions (dotted) are also depicted.

The fields are also stronger at the surface because of lower electron density, and the ions from that region are accelerated more. The hottest trapped electrons are found mostly in the center of the cluster. At $t=160$ fs, 1200 carbon ions are in the charge state 4+, 250 in state 5+, and they all fill the entire volume of, at that time, 5 nm radius (see Fig. 10). 25 fs later, the cluster radius is twice as large, the C^{4+} ions (in number of 470) are located in a shell at least 5 nm far from the cluster center, and the 700 C^{5+} ions are now continuously distributed up to a distance of 8 nm from the center. From the numerical calculations it looks like the ionization of the K shell takes place predominantly in the core of the cluster, which is more or less neutral, and the ions originating there are not accelerated very much. At this time, 185 fs, the average ionic charge state is already 5+, the positive-charge density slightly exceeds the negative one [Fig. 9(a)], while the hydrodynamic pressure drives the cluster into expansion.

The differences between the numerical results and the experimental ones can be explained by the differences between the experimental conditions and the assumptions we made in the simulations, mainly regarding the focal intensity distribution, the cluster size, and the cluster structure and composition. Note that the cluster used in the calculation still contains two orders of magnitude fewer particles that the propane clusters in the experiment. All quantities are expected to approach some asymptotic value with cluster size, though. Even if the simulation does not reproduce exactly the experimental results, it still gives a valuable insight into the way the explosion occurs.

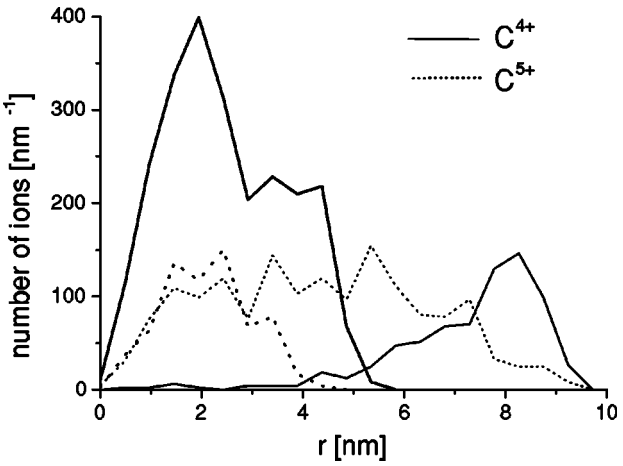

FIG. 10. Number of ions as a function of the distance from the center of the cluster, at $t=160$ fs (thick lines) and at $t=185$ fs (thin lines).

V. CONCLUSIONS

We have reported in this paper some results obtained in an experiment of infrared-laser irradiation of clusters of propane (50 000 molecules on average) and carbon dioxide (4500 molecules). The determination of the cluster size was done using the Rayleigh-scattering technique, an indirect method of measurement, yet the only one available in the absence of mass-spectroscopy means. Ions of C^{5+} and O^{6+}, with kinetic energies up to 2 keV, were produced starting from 1.5×10^{14} W/cm^2, a much lower intensity than is required for tunneling ionization. Numerical simulations confirm the occurrence of resonant heating of the electrons by absorption of laser energy and the importance of this process in the production of highly charged ions by electron collisional ionization. The simulations indicate that the hydrodynamic pressure triggers the process of expansion, but it is the Coulomb repulsion that is responsible for the high energies of the ions.

At 800 nm, it proved to be very difficult to obtain completely stripped carbon ions, even when very large clusters were used. It was not possible to obtain only high-charge states because of the large dominace of low intensities in the focus that produced a lot of triply or quadruply charged carbon ions. It might be interesting to do this experiment at a single intensity, using a spatially shaped focus, because the calculations indicate that under this condition it is possible to create predominantly highly charged ions.

ACKNOWLEDGMENTS

This work was part of the research program of FOM (Fundamental Research on Matter), which is subsidized by NWO (Netherlands Organization for the Advancement of Research).

[1] L. F. DiMauro and P. Agostini, Adv. At., Mol., Opt. Phys. **35**, 79 (1995).
[2] L. V. Keldysh, Sov. Phys. JETP **20**, 1307 (1965).
[3] M. Protopapas, C. H. Keitel, and P. L. Knight, Rep. Prog. Phys. **60**, 389 (1997).
[4] A. McPherson, B. D. Thompson, A. B. Borisov, K. Boyer, and C. K. Rhodes, Nature (London) **370**, 631 (1994).
[5] T. Ditmire, T. Donnelly, R. W. Falcone, and M. D. Perry, Phys. Rev. Lett. **75**, 3122 (1995).
[6] S. Dobosz, M. Leszius, M. Schmidt, P. Meynadier, M. Perdrix, and D. Normand, Phys. Rev. A **56**, R2526 (1997).
[7] T. Ditmire, J. Zweiback, V. P. Yanovsky, T. E. Cowan, G. Hays, and K. B. Wharton, Nature (London) **398**, 489 (1999).
[8] T. Ditmire, J. W. G. Tisch, E. Springate, M. B. Mason, N. Hay, R. A. Smith, J. Marangos, and M. H. R. Hutchinson, Nature (London) **386**, 54 (1997).
[9] T. Ditmire, J. W. G. Tisch, E. Springate, M. B. Mason, N. Hay, J. P. Marangos, and M. H. R. Hutchinson, Phys. Rev. Lett. **78**, 2732 (1997).
[10] T. Ditmire, E. Springate, J. W. G. Tisch, Y. L. Shao, M. B. Mason, N. Hay, J. P. Marangos, and M. H. R. Hutchinson, Phys. Rev. A **57**, 369 (1998).
[11] Y. L. Shao, T. Ditmire, J. W. G. Tisch, E. Springate, J. P. Marangos, and M. H. R. Hutchinson, Phys. Rev. Lett. **77**, 3343 (1996).
[12] B. D. Thompson, A. McPherson, K. Boyer, and C. K. Rhodes, J. Phys. B **27**, 4391 (1994).
[13] A. McPherson, T. S. Luk, B. D. Thompson, A. B. Borisov, O. B. Shiryaev, X. Chen, K. Boyer, and C. K. Rhodes, Phys. Rev. Lett. **72**, 1810 (1994).
[14] E. M. Snyder, S. A. Buzza, and A. W. Castleman Jr., Phys. Rev. Lett. **77**, 3347 (1996).
[15] C. Rose-Petruck, K. J. Schafer, K. R. Wilson, and C. P. J. Barty, Phys. Rev. A **55**, 1182 (1997).
[16] T. Ditmire, Phys. Rev. A **57**, R4049 (1998).
[17] T. Ditmire, T. Donnelly, A. M. Rubenchik, R. W. Falcone, and M. D. Perry, Phys. Rev. A **53**, 3379 (1996).
[18] J. Zweiback, T. Ditmire, and M. D. Perry, Phys. Rev. A **59**, R3166 (1999).
[19] M. Lezius, S. Dobosz, D. Normand, and M. Schmidt, Phys. Rev. Lett. **80**, 261 (1998).
[20] J. V. Ford, Q. Zhong, L. Poth, A. W. Castleman, Jr., J. Chem. Phys. **110**, 6257 (1999).
[21] E. Springate, N. Hay, J. W. G. Tisch, M. B. Mason, T. Ditmire, M. H. R. Hutchinson, and J. P. Marangos, Phys. Rev. A **61**, 063201 (2000).
[22] R. C. Constantinescu, S. Hunsche, H. B. van Linden van den Heuvell, H. G. Muller, C. LeBlanc, and F. Salin, Phys. Rev. A **58**, 4637 (1998).
[23] O. F. Hagena and W. Obert, J. Chem. Phys. **56**, 1793 (1972).
[24] O. F. Hagena, Surf. Sci. **106**, 101 (1981).
[25] O. F. Hagena, Z. Phys. D: At., Mol. Clusters **4**, 291 (1987).
[26] O. F. Hagena, Rev. Sci. Instrum. **63**, 2374 (1991).
[27] O. F. Hagena, Phys. Fluids **17**, 894 (1974).
[28] J. Farges, M. F. de Feraudy, B. Raoult, and G. Torchet, J. Chem. Phys. **84**, 3491 (1986).
[29] J. Wörmer, V. Guzielski, J. Stapelfeldt, and T. Möller, Chem. Phys. Lett. **159**, 321 (1989).
[30] D. R. Miller, in *Atomic and Molecular Beam Methods*, edited by G. Scoles (Oxford University Press, Oxford, 1988), Vol. I, p. 14.
[31] W. Lotz, Z. Phys. **216**, 241 (1968).
[32] I. Last and J. Jortner, Phys. Rev. A **62**, 013201 (2000).
[33] N. B. Delone and V. P. Krainov, Phys. Usp. **41**, 469 (1998).